Cellular Imaging

International Edition: DOI: 10.1002/anie.201707042
German Edition: DOI: 10.1002/ange.201707042

Conjugated Polymer with Intrinsic Alkyne Units for Synergistically Enhanced Raman Imaging in Living Cells

Shengliang Li[+], Tao Chen[+], Yunxia Wang, Libing Liu, Fengting Lv, Zhiliang Li, Yanyi Huang, Kirk S. Schanze,* and Shu Wang**

Abstract: *Development of Raman-active materials with enhanced and distinctive Raman vibrations in the Raman-silent region (1800–2800 cm^{-1}) is highly required for specific molecular imaging of living cells with high spatial resolution. Herein, water-soluble cationic conjugated polymers (CCPs), poly(phenylene ethynylene) (PPE) derivatives, are explored for use as alkyne-state-dependent Raman probes for living cell imaging due to synergetic enhancement effect of alkyne vibrations in Raman-silent region compared to alkyne-containing small molecules. The enhanced alkyne signals result from the integration of alkyne groups into the rigid backbone and the delocalized π-conjugated structure. PPE-based conjugated polymer nanoparticles (CPNs) were also prepared as Raman-responsive nanomaterials for distinct imaging application. This work opens a new way into the development of conjugated polymer materials for enhanced Raman imaging.*

Advances in optical microscopy in the past decades have tremendously promoted the development of biomedical fields, such as drug discovery, disease diagnosis, and therapeutics.[1] In particular, originally exploited as a label-free imaging technique, Raman microscopy has become an emerging tool for cell imaging, mainly because it is capable of visualizing specific vibrations that provide information about molecular fingerprint.[2] Recent advances in confocal Raman microscopy have enabled high-contrast Raman images of living cells.[3] However, most of the current Raman imaging agents are difficult to acquire high-contrast Raman images of cells owning to the intrinsically small cross-section of Raman scattering and the interference from the endogenous background Raman signal of cells. Thus, the development of probe materials possessing a strong Raman signal in the Raman-silent region of cells (1800–2800 cm^{-1}) is highly required. Recent studies have demonstrated that bioorthogonal alkyne groups as specific Raman probes exhibit strong Raman scattering at about 2100–2200 cm^{-1}, and have been exploited for imaging DNA, lipid, protein, and glycan in living cells.[4]

Conjugated polymers (CPs) with large π-electronic delocalized backbones and prominent photo-electronic properties, have emerged as a new class of versatile functional materials for light-harvesting applications, such as organic solar cells,[5] field-effect transistors,[6] and light-emitting diodes.[7] Moreover, the CPs can effectively coordinate the action of a large number of fluorescent units with energy transfer mechanisms, which could enhance the light-harvesting and light-amplifying properties, thus they have recently been widely used for optical imaging,[8] optical biosensors[9] and phototherapy.[10] However, exploration of conjugated polymers as a new imaging modality, especially Raman scattering and molecular fingerprint, is still in its infancy. In this work, we explored conjugated polymers as new Raman materials and demonstrated their advantages for Raman imaging of living cells. Compared to previously reported alkyne-containing small molecules, water-soluble cationic poly(phenylene ethynylene) (PPE) derivatives exhibited dramatically enhanced alkyne vibrations in the Raman-silent region of cells. Utilizing the enhancement effect of alkyne vibrations, cationic PPE was specifically visualized in living cells by using the alkyne fingerprint. PPE-based conjugated polymer nanoparticles (CPNs) were also prepared and functionalized with cell penetrating peptides Tat for the enhanced living cell imaging. Therefore, PPE derivatives are good candidates as new Raman-responsive materials with enhanced signal and persistent in silent-region of living biological system.

Three cationic conjugated polymers (PFP, PPV, and PPE) were employed in this work and the spontaneous Raman spectra were studied by using confocal Raman microscopy. As shown in Figure 1, all of the three CPs show various vibrational bands at the fingerprint region from 1000–1800 cm^{-1} upon excitation of 785 nm laser. Notably, only PPE exhibits a strong and narrow Raman peak around 2200 cm^{-1}, which represents the carbon–carbon triple bond stretching and location in Raman-silent region of cells. The positon of this alkyne specific Raman peak did not change upon irradiation under excitation with different wavelengths (532, 633, and 785 nm) (Figure S1 in the Supporting Information). We also investigated the stability of this alkyne Raman signal, and the results showed that alkyne Raman scattering of PPE maintained similar strength even after irradiation by a 785 nm laser for 30 min (Figure S2). These findings strongly suggest that

[*] Dr. S. Li,[+] Dr. Y. Wang, Dr. L. Liu, Dr. F. Lv, Prof. S. Wang
Beijing National Laboratory for Molecular Sciences, Key Laboratory of Organic Solids, Institute of Chemistry, Chinese Academy of Sciences, Beijing 100190 (P. R. China)
E-mail: wangshu@iccas.ac.cn
Dr. T. Chen,[+] Prof. Y. Huang
Biodynamic Optical Imaging Center, College of Engineering, Peking University, Beijing 100871 (P. R. China)
E-mail: yanyi@pku.edu.cn
Dr. Z. Li, Prof. K. S. Schanze
Department of Chemistry, University of Texas at San Antonio
San Antonio, TX 78249 (USA)
E-mail: Kirk.Schanze@utsa.edu
[+] These authors contributed equally to this work.

Supporting information for this article can be found under: https://doi.org/10.1002/anie.201707042.

 © 2017 Wiley-VCH Verlag GmbH & Co. KGaA, Weinheim

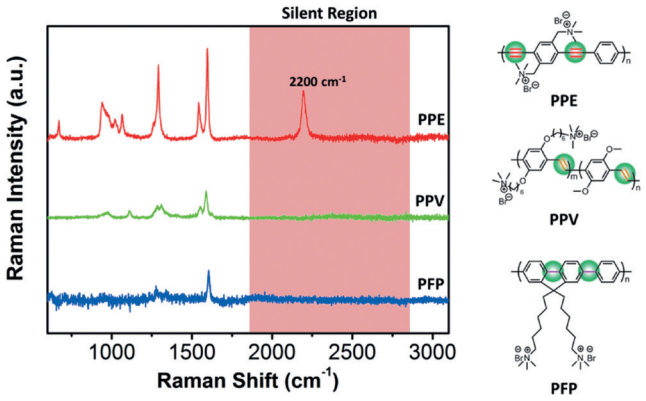

Figure 1. Raman shifts and chemical structures of three cationic conjugated polymers used in this work.

PPE derivatives have strong alkyne vibrational signal in Raman-silent region of cells, and hold the excellent promise as Raman probes for live-cell Raman imaging.

To expand this strategy, we chose six PPE derivatives with different types of pendants to further test their Raman-responsive behaviors (see their chemical structures in Figure 2a). Their photophysical properties were performed and summarized in Figure S3 and Table S1. As expected, all six PPE derivatives exhibit a sufficiently strong and narrow spontaneous Raman signal at 2200 cm^{-1}, the signature vibration of the alkyne groups (Figure 2b). It is well known that the intrinsically weak Raman signal is the major roadblock for living cell Raman imaging. Conjugation of an alkyne group to aromatic ring can effectively enhance the Raman signal.[5] It is expected that alkyne-containing conjugated backbone in PPE can enhance the alkyne vibrations in Raman-silent region of cells through aromatic rings conjugation and the delocalized π-conjugated structure. Initially, we employed a previous method to evaluate the Raman enhancement effect of PPE derivatives.[11] Owing to its wide application in live-cell Raman imaging, EdU (5-ethynyl-2′-deoxyuridine) was chosen as standard. Other alkynyl and PPE derivatives were mixed with EdU in dimethyl sulfoxide (DMSO) followed by the examination of Raman spectra. The relative Raman intensity versus EdU (RIE) was obtained from the peak area of the alkyne peaks. As shown in Figure 2c, both diphenylacetylene (DPE)[12] and PPE derivatives exhibit stronger Raman intensity in alkyne vibrations compared with EdU, while butyne and phenylacetylene do not show an obvious signal under the same conditions. These results are consistent with previous studies that aromatic rings can effectively enhance the alkyne Raman signal. Note that the PPE derivatives show much stronger alkyne Raman scattering (approximately 2.8 times greater) than DPE (Figures S4–S8). Thus, PPE possesses synergetic enhancement effect on alkyne Raman scattering, highlighting the great promise as excellent Raman probe for imaging.

Since both PPE derivatives P5 and P6 exhibit strong Raman activity at the Raman-silent region of cells, they were employed as vibrational probes for living cell imaging under Raman microscopy. Raman spectra of P5 and P6 were mapped in living cells (Figure 3a), and dual-color Raman imaging of HeLa cells was acquired with the employment of 2200 cm^{-1} for alkyne and 2850 cm^{-1} for lipid (CH_2) (Figure 3b). Furthermore, the Raman spectra extracted from

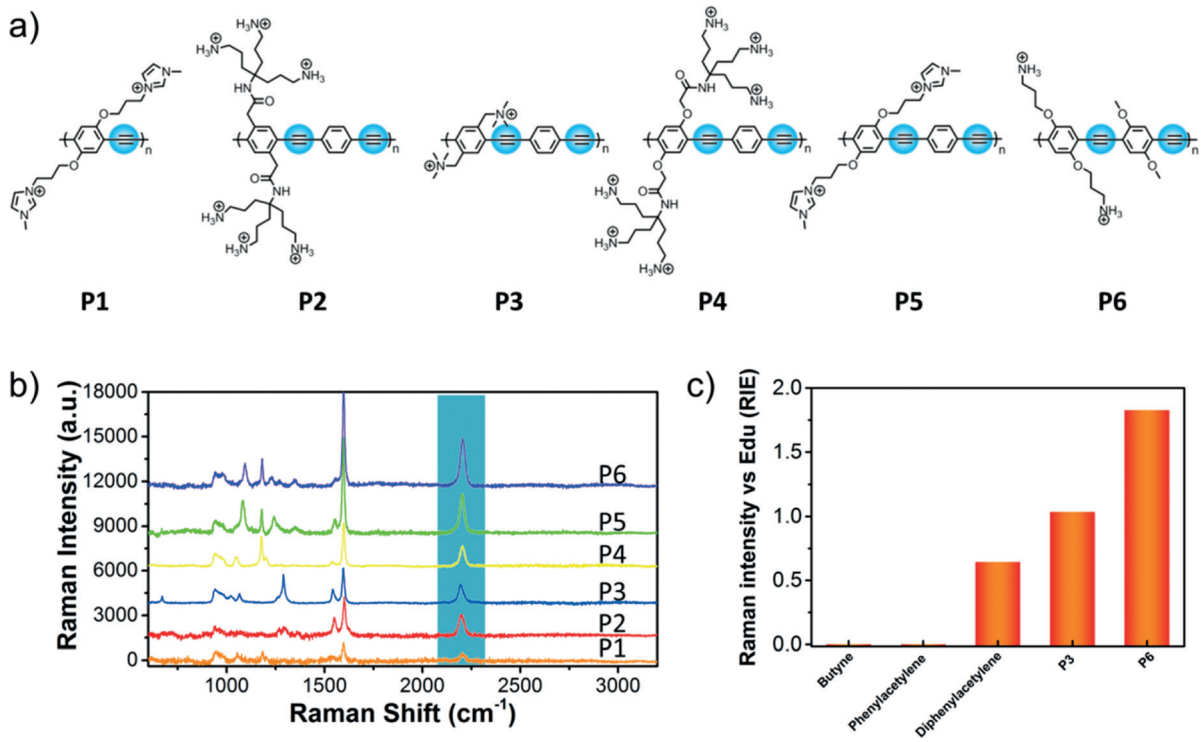

Figure 2. Raman shift/intensity relationship of PPE derivatives. a) The chemical structures of PPE derivatives. b) Spontaneous Raman spectra. c) Relative Raman intensity of alkynyl and PPE derivatives versus EdU (RIE).

© 2017 Wiley-VCH Verlag GmbH & Co. KGaA, Weinheim

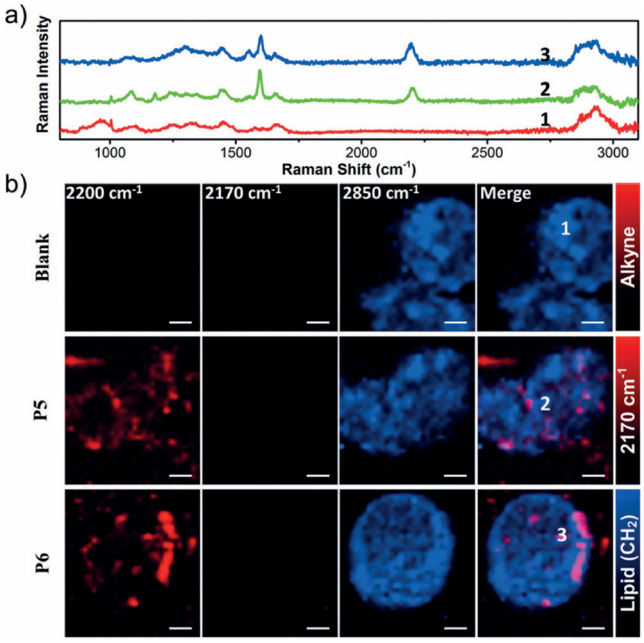

Figure 3. a) Raman spectra of P5 and P6 in living cells, which were taken at three locations in cells as indicated in Raman images of Figure 3b. b) Representative Raman images of HeLa cells treated with or without P5 and P6 (10 μM in repeat units) for 6 h. Scale bars: 5 μm.

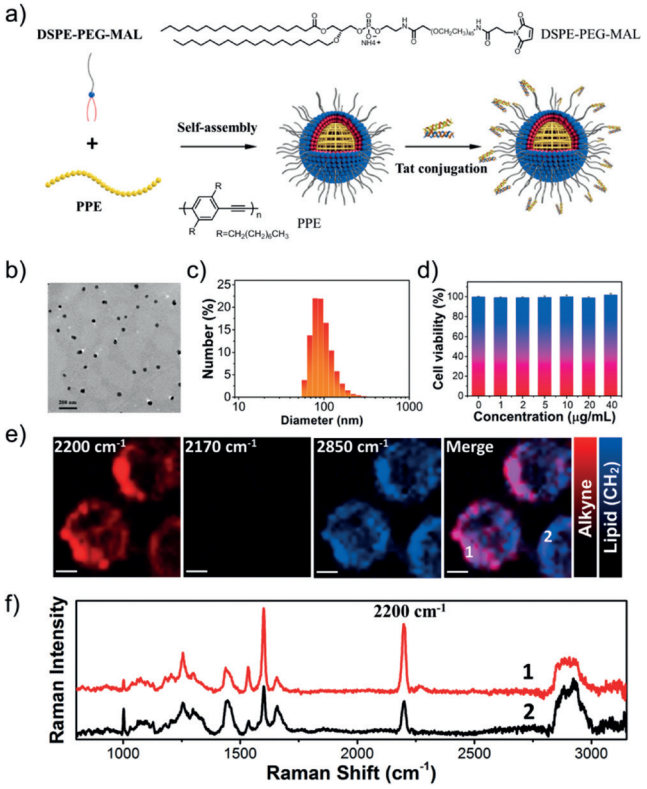

Figure 4. a) Schematic illustration for preparation of Tat-PPE NPs. b) TEM image of Tat-PPE NPs. c) Representative DLS profiles of Tat-PPE NPs. d) Relative viabilities of HeLa cells after incubation with various concentrations of Tat-PPE NPs for 24 h. e) Living cell Raman images of HeLa cells treated with Tat-PPE NPs (10 μg mL^{-1}) for 6 h. Scale bars: 5 μm. f) Representative Raman spectra at two locations in living cell as indicated in the Raman image of Figure 4d.

living cells show that the cells treated with P5 and P6 feature a specific alkyne peak around 2200 cm^{-1} in the Raman-silent region of cells. No alkyne signal around 2200 cm^{-1} was observed in the control group, indicating the superiority of PPE in interference-free Raman imaging of living cells. The biocompatibility of P5 and P6 were confirmed by MTT assay (Figure S9). The Raman images of alkyne at 2200 cm^{-1} show that P5 and P6 are widely distributed in the cell cytoplasm. Advantageously, the off-peak measurement (2170 cm^{-1}) exhibits negligible signal in cells, providing clear background of the images. These results collectively demonstrate the advantage of the PPE for living cell Raman imaging.

Prompted by the results on Raman imaging of the PPE in living cells, we prepared PPE-based nanoparticles for distinct imaging application. The nano-precipitation of hydrophobic PPE with DSPE-PEG$_{2000}$-Mal was performed to obtain nanoparticles as schematically illustrated in Figure 4a. To enhance the cell uptake of nanoparticles, the resulting PPE NPs were further modified with Tat peptide (RKKRRQRRRC) through conjugation between maleimide groups on the nanoparticle surface and thiol groups at the C-terminus of the Tat peptide. The spherical shape of Tat-PPE NPs was confirmed by using transmission electron microscopy (TEM) (Figure 4b). Moreover, dynamic light scattering (DLS) was used to confirm their narrow size distribution with the average size of 96 ± 1.4 nm (Figure 4c), which is similar to that of PPE NPs (Figure S10). In addition, Tat-PPE NPs possess positive zeta potentials of 25 ± 2.1 mV in PBS (pH 7.4), which is preferred for cell uptake (Figure S11). Raman spectra of Tat-PPE NPs were then investigated by confocal laser Raman microscopy. The result shows that Tat-PPE NPs exhibit evident alkyne peak around 2200 cm^{-1}, which is similar to PPE (Figure S12). Notably, no significant cytotoxicity for HeLa cells was observed after incubation with various concentrations of Tat-PPE NPs for 24 h, highlighting the excellent biocompatibility of the new Raman nano-probe (Figure 4d). Dual-color Raman imaging of HeLa cells was employed. After treatment with Tat-PPE NPs for 6 h, HeLa cells exhibit a strong signal of the alkyne in the cytoplasm, which reveals the intracellular distribution of Tat-PPE NPs (Figure 4e). Meanwhile, fluorescence imaging was used to observe the distribution of Tat-PPE NPs as well, and it is similar to the living cell Raman imaging (Figure S13). Importantly, for Tat-PPE NPs, the off-peaking measurement (2170 cm^{-1}) also shows a minimal Raman signal in cells, while with a specific alkyne peak around 2200 cm^{-1}, highlighting the superiority of Raman imaging using Tat-PPE NPs (Figure 4e and f). In consideration of the synergetic-enhancement effect of alkyne vibrations in CPNs and good performance of plasmonic SERS-nanotag,[13] plasmonic-PPE NPs could further enhance the alkyne vibrations for live cell imaging.

In summary, we demonstrated for the first time that poly(phenylene ethynylene) (PPE) derivatives can be used as Raman-active materials with synergetic-enhancement effect of alkyne vibrations in Raman-silent region for live cell imaging. The PPE provides three main advantages compared with those alkyne-containing small molecules: 1) alkyne unit

 © 2017 Wiley-VCH Verlag GmbH & Co. KGaA, Weinheim

is conjugated into the middle of two aromatic rings, which can effectively enhance the Raman intensity of alkyne vibrations; 2) alkyne-containing backbone of conjugated polymer exhibits substantial π-conjugation, which is advantageous to enhance Raman scattering signal; 3) it shows a strong signal in Raman-silent region of cells, obviously enhancing the contrast of Raman imaging. PPE-based nanoparticles were also prepared with excellent biocompatibility and functionalization, which is advantageous as Raman-responsive nanomaterials for distinct imaging application. This work exhibits the good potential of conjugated polymer materials for enhanced Raman activity, and also expands the use of conjugated polymers in biological imaging.

Acknowledgements

The authors are grateful to the National Natural Science Foundation of China (Nos. 21533012, 91527306, 21661132006, 21525521), the China Postdoctoral Science Foundation (2015M571131, 2016T90138) and the Strategic Priority Research Program of the Chinese Academy of Sciences (XDA09030306).

Conflict of interest

The authors declare no conflict of interest.

Keywords: living cells · nanoparticles · poly(phenylene ethynylene) · Raman imaging

How to cite: *Angew. Chem. Int. Ed.* **2017**, *56*, 13455–13458
Angew. Chem. **2017**, *129*, 13640–13643

[1] a) R. Weissleder, *Science* **2006**, *312*, 1168–1171; b) S. S. Gambhir, *Nat. Rev. Cancer* **2002**, *2*, 683–693; c) S. R. Mudd, R. A. Comley, M. Bergstrom, K. D. Holen, Y. Luo, S. Carme, G. B. Fox, L. Martarello, J. D. Beaver, *Drug Discov. Today* **2017**, *22*, 140–147; d) E. Betzig, J. Trautman, T. Harris, J. Weiner, R. Kostelak, *Science* **1991**, *251*, 1468–1470.

[2] a) H. Abramczyk, B. Brozek-Pluska, *Chem. Rev.* **2013**, *113*, 5766–5781; b) L. A. Lane, X. Qian, S. Nie, *Chem. Rev.* **2015**, *115*, 10489–10529; c) S. Keren, C. Zavaleta, Z. Cheng, A. de La Zerda, O. Gheysens, S. Gambhir, *Proc. Natl. Acad. Sci. USA* **2008**, *105*, 5844–5849; d) C. Krafft, I. Schie, T. Meyer, M. Schmitt, J. Popp, *Chem. Soc. Rev.* **2016**, *45*, 1819–1849; e) Z. Liu, X. Li, S. M. Tabakman, K. Jiang, S. Fan, H. Dai, *J. Am. Chem. Soc.* **2008**, *130*, 13540–13541; f) K. V. Kong, Z. Lam, W. D. Goh, W. K. Leong, M. Olivo, *Angew. Chem. Int. Ed.* **2012**, *51*, 9796–9799; *Angew. Chem.* **2012**, *124*, 9934–9937; g) I. Pence, A. Mahadevan-Jansen, *Chem. Soc. Rev.* **2016**, *45*, 1958–1979.

[3] a) W. Tipping, M. Lee, A. Serrels, V. Brunton, A. Hulme, *Chem. Soc. Rev.* **2016**, *45*, 2075–2089; b) C. W. Freudiger, W. Min, B. G. Saar, S. Lu, G. R. Holtom, C. He, J. C. Tsai, J. X. Kang, X. S. Xie, *Science* **2008**, *322*, 1857–1861; c) C. M. Girish, A. Sasidharan, G. S. Gowd, S. Nair, M. Koyakutty, *Adv. Healthcare Mater.* **2013**, *2*, 1489–1500.

[4] a) L. Wei, F. Hu, Y. Shen, Z. Chen, Y. Yu, C.-C. Lin, M. C. Wang, W. Min, *Nat. Methods* **2014**, *11*, 410–412; b) M. Xiao, L. Lin, Z. Li, J. Liu, S. Hong, Y. Li, M. Zheng, X. Duan, X. Chen, *Chem. Asian J.* **2014**, *9*, 2040–2044; c) L. Lin, X. Tian, S. Hong, P. Dai, Q. You, R. Wang, L. Feng, C. Xie, Z. Q. Tian, X. Chen, *Angew. Chem. Int. Ed.* **2013**, *52*, 7266–7271; *Angew. Chem.* **2013**, *125*, 7407–7412; d) H. Yamakoshi, K. Dodo, M. Okada, J. Ando, A. Palonpon, K. Fujita, S. Kawata, M. Sodeoka, *J. Am. Chem. Soc.* **2011**, *133*, 6102–6105; e) Z.-L. Song, Z. Chen, X. Bian, L.-Y. Zhou, D. Ding, H. Liang, Y.-X. Zou, S.-S. Wang, L. Chen, C. Yang, *J. Am. Chem. Soc.* **2014**, *136*, 13558–13561.

[5] C. Liu, K. Wang, X. Gong, A. J. Heeger, *Chem. Soc. Rev.* **2016**, *45*, 4825–4846.

[6] N. Stutzmann, R. H. Friend, H. Sirringhaus, *Science* **2003**, *299*, 1881–1884.

[7] M. Gross, D. C. Müller, H.-G. Nothofer, U. Scherf, D. Neher, C. Bräuchle, K. Meerholz, *Nature* **2000**, *405*, 661–665.

[8] a) A. W. Thomas, Z. B. Henson, J. Du, C. A. Vandenberg, G. C. Bazan, *J. Am. Chem. Soc.* **2014**, *136*, 3736–3739; b) J. Yu, C. Wu, X. Zhang, F. Ye, M. E. Gallina, Y. Rong, I. C. Wu, W. Sun, Y. H. Chan, D. T. Chiu, *Adv. Mater.* **2012**, *24*, 3498–3504; c) K. Pu, A. J. Shuhendler, J. V. Jokerst, J. Mei, S. S. Gambhir, Z. Bao, J. Rao, *Nat. Nanotechnol.* **2014**, *9*, 233–239.

[9] a) J. Song, J. Zhang, F. Lv, Y. Cheng, B. Wang, L. Feng, L. Liu, S. Wang, *Angew. Chem. Int. Ed.* **2013**, *52*, 13020–13023; *Angew. Chem.* **2013**, *125*, 13258–13261; b) B. Xing, T. Li, Z. Tang, L. Jiao, S. Ge, X. Qiang, J. OuYang, *GMR Genet. Mol. Res.* **2015**, *14*, 4532–4540; c) F. Feng, Y. Tang, S. Wang, Y. Li, D. Zhu, *Angew. Chem. Int. Ed.* **2007**, *46*, 7882–7886; *Angew. Chem.* **2007**, *119*, 8028–8032; d) Q. Wen, L. Liu, Q. Yang, F. Lv, S. Wang, *Adv. Funct. Mater.* **2013**, *23*, 764–769.

[10] a) C. Xing, Q. Xu, H. Tang, L. Liu, S. Wang, *J. Am. Chem. Soc.* **2009**, *131*, 13117–13124; b) B. Wang, H. Yuan, Z. Liu, C. Nie, L. Liu, F. Lv, Y. Wang, S. Wang, *Adv. Mater.* **2014**, *26*, 5986–5990; c) Y. Lyu, Y. Fang, Q. Miao, X. Zhen, D. Ding, K. Pu, *ACS Nano* **2016**, *10*, 4472–4481.

[11] H. Yamakoshi, K. Dodo, A. Palonpon, J. Ando, K. Fujita, S. Kawata, M. Sodeoka, *J. Am. Chem. Soc.* **2012**, *134*, 20681–20689.

[12] a) L. Xie, X. Ling, Y. Fang, J. Zhang, Z. Liu, *J. Am. Chem. Soc.* **2009**, *131*, 9890–9891; b) X. Ling, W. Fang, Y.-H. Lee, P. T. Araujo, X. Zhang, J. F. Rodriguez-Nieva, Y. Lin, J. Zhang, J. Kong, M. S. Dresselhaus, *Nano Lett.* **2014**, *14*, 3033–3040; c) S. He, K.-K. Liu, S. Su, J. Yan, X. Mao, D. Wang, Y. He, L.-J. Li, S. Song, C. Fan, *Anal. Chem.* **2012**, *84*, 4622–4627.

[13] a) P. Rivera Gil, C. Vazquez-Vazquez, V. Giannini, M. P. Callao, W. J. Parak, M. A. Correa-Duarte, R. A. Alvarez-Puebla, *Angew. Chem. Int. Ed.* **2013**, *52*, 13694–13698; *Angew. Chem.* **2013**, *125*, 13939–13943; b) S. Ma, Q. Li, Y. Yin, J. Yang, D. Liu, *Small* **2017**, *13*, 1603340; c) N. Feliu, X. Sun, R. A. A. Puebla, W. J. Parak, *Langmuir* **2017**, *33*, 6639–6646.

Manuscript received: July 11, 2017
Accepted manuscript online: August 29, 2017
Version of record online: September 19, 2017

 © 2017 Wiley-VCH Verlag GmbH & Co. KGaA, Weinheim